ISSN 2179-3956

INFLUENCE OF TEXTURED SURFACE ARRANGEMENT ON HYDRODYNAMIC JOURNAL BEARING PERFORMANCE [1]

Nacer Tala Ighil [2]
Michel Fillon [3]
Patrick Maspeyrot [3]

Abstract
A progressive interest is granted to the textured surfaces in a journal bearing. The use of surfaces with certain shapes and dispositions of textures can be an effective approach to improve the performance of hydrodynamic bearings. This paper presents the numerical approach used to analyze the effect of cylindrical texture form on the characteristics of a hydrodynamic contact. The results obtained show that the most important characteristics of the contact like minimal film thickness, maximal pressure, axial fluid flow and friction torque can be improved through an appropriate choice of textures distribution on the contact surface.
Keywords: Textures; Hydrodynamic lubrication; Journal bearing.

[1] *Technical contribution to the First International Brazilian Conference on Tribology – TriboBr-2010, November, 24th-26th, 2010, Rio de Janeiro, RJ, Brazil.*
[2] *Centre de Recherche Scientifique et Technique en Soudage et Contrôle (CSC), Route de Dely-Ibrahim BP 64, Chéraga, Alger -Algerie-. Institut Pprime, Dpt Génie Mécanique et Systèmes Complexes, SP2MI, Bd Pierre etMarie Curie, BP 30179, 86962 Futuroscope Chasseneuil Cedex, France.*
[3] *Institut Pprime, Dpt Génie Mécanique et Systèmes Complexes, SP2MI, Bd Pierre etMarie Curie, BP 30179, 86962 Futuroscope Chasseneuil Cedex, France.*

ISSN 2179-3956

1 INTRODUCTION

The hydrodynamic bearings are frequently used in wide range of applications and mechanisms since long. Actually, little is understood about the subtle effects of variations of a journal bearing's profile upon its performance. The surface texturing is expected to make an important contribution to future technologies of bearing. Surface texturing is claiming progressively more attention and is expected to be an important component in future bearing structure design

Many works[1-8] were dedicated to the study of the random influence roughness on the hydrodynamic journal bearing performance; the conclusion was that the roughness influences the bearing performance. The random roughness in hydrodynamic bearings may be introduced due to the presence of dust, additives in the lubricant and wear while the roughness may be random or deterministic nature.

As demonstrated by the authors,[9,10] the deterministic roughness which is known as surface texture was introduced deliberately on the bearings with the help of micro fabrication techniques. By means of new technology like laser surface texturing,[11] it is now possible to produce controlled microgeometries (textures) on journal bearing surfaces to improve the overall tribological performance including the friction reduction, the reliability improvement, the severity conditions increase and the energy consumption lowering.

Tonder[12] pointed out that by introducing a series of dimples or roughness at inlet of a sliding surface we can generate extra pressure and thus support higher load, this has also been confirmed by Cupillard, Glavatskih, and Cervantes.[13] Kovalchenko et al.[14] showed that laser texturing expanded the contact parameters in terms of load and speed for hydrodynamic lubrication. Siripuram and Stephens[15] presents a numerical study of micro-asperities effects with different shapes in sliding surface lubrication when hydrodynamic films are found. The minimum coefficient of friction for all shapes is found to occur at an asperity area fraction of 0.2 for positive asperities and 0.7 for negative asperities. Some other and recent studies[16-20] have established that the surface texture geometry such as texture depth, width, number of textures and location of textures influence the bearing performance.

In others studies, Navier-Stokes equations have been solved for the flow between two parallel surfaces, one smooth and one having a single surface pocket. They showed that the pressure generating effect of surface texture in full film operation might result from convective inertia. Piezo-viscosity may play a role in heavily loaded lubricated contacts. Thus, in local converging regions the pressure rise may be larger than the pressure drop in diverging regions. According to De Kraker et al.,[21] the use of a Reynolds equation to study the effects of texture will be valid if dimple depth is greater than minimum film thickness of the lubricant in the fluid film lubrication. Cupillard, Glavatskih and Cervantes[22] have found that the mechanism of pressure build up in a convergent gap between two sliding surfaces due to texture is similar to that obtained with convergence ratio variation for smooth surfaces. The same author[23] found that there is an optimal texture depth, greater than the critical depth, which gives the maximum load carrying capacity. Above this depth, a global recirculation zone occurs in each dimple, leading to a loss in the load-carrying capacity. In non-cavitated hydrodynamic contacts where Reynolds assumptions hold true, Buscaglia, Ciuperca and Jai[24] shown that full texturing has a negative impact on both hydrodynamic lift and viscous friction. The

ISSN 2179-3956

positive texture effects observed in fully textured parallel sliders is explained by two theories. The first one considers the cavitation phenomena as the source of these positive effects. Accordingly, the presence of dimples creates an alternation of converging and diverging film regions, in which the pressure varies between a positive value in the lubricated regions and the vaporization pressure in the cavitated regions. Consequently, an overall positive resultant is obtained.(25) A second theory suggests that the load capacity generated in fully textured parallel sliders is caused by inertia effects (convective inertia). It was recently shown that this theory is inaccurate and that inertia effects have, in general, a negative influence over the hydrodynamic performance.(26) Consequently, cavitation emerges as the main mechanism leading to the observed increased lift and reduced friction in fully textured parallel sliders. Recently, Dobrica et al.(27) conclude that:

- Full texturing is unable to generate hydrodynamic lift in parallel sliders, except when the dimples are placed at the slider inlet (the generated lift is minimal). In convergent plane-inclined sliders, full texturing has negative effects.
- In parallel sliders, starting partial texturing at the inlet generates significant hydrodynamic lift. In plane-inclined sliders with low global film convergence, partial texturing provides soft performance improvements. In highly convergent sliders, texturing has minimal effects.

Endeavours were made in several studies to determine the optimal texturing parameters that would minimize friction or maximize the fluid film thickness. One emerging conclusion of these studies is that partial texturing leads to better performance than full texturing.

In the present work therefore, deterministic surface texture is used to study the influence of textures location on the bearing surface. The surface analysis, used in hydrodynamic lubrication, requires detailed statements of surface; a grid refined of this one and an important computing power. A numerical approach is used in order to give a description of the textures location effect on the most important characteristics in a hydrodynamic bearing. Through a wise choice of the textures arrangement on one of the bearing surfaces, its performance can be improved. The bearing surface is textured with cylindrical dimples.

2 PROBLEM FORMULATIONS

In a hydrodynamic lubrication problem, the governing equations in a full hydrodynamic lubrication region can be described by the well-known Reynolds' equation. For Cartesian coordinates, when the thickness of the lubricant film h is in the direction of the y axis (figure 1), the pressure in the lubricating film for a journal operating at steady state, is governed by the following equation:(28)

$$\frac{\partial}{\partial\theta}\left(h^3\frac{\partial P}{\partial\theta}\right)+\left(\frac{R}{L}\right)^2\frac{\partial}{\partial Z}\left(h^3\frac{\partial P}{\partial Z}\right)=6\mu R^2\left[\left(\omega_2-\omega_1\right)\frac{\partial h}{\partial\theta}\right] \quad (1)$$

In equation (1), P is the lubricant pressure, h is the film thickness. Equation (2) describes the film thickness h which can be written as follows.

$$h = h_{smooth}(\theta) + \Delta h\,(\theta,Z) \quad (2)$$

ISSN 2179-3956

It is a known fact that the lubricant film thickness $h_{smooth}=C(1+\varepsilon.\cos\theta)$ for smooth bearing (without textures) is dependent upon radial clearance C, eccentricity ratio ε and the angular position θ. In the equation above, $\Delta h(\theta,Z)$ is the film thickness variation due to the textured surface (Figure 1b).

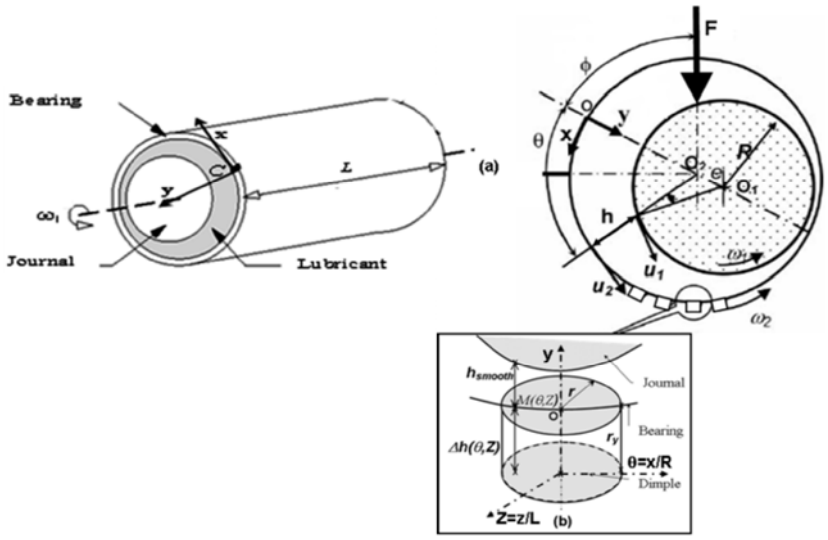

Figure 1. System of journal bearing; (a) a cross section of the journal-bearing; (b) texture form.

The boundary conditions, known as Reynolds boundary conditions, are used to determine the rupture zone of the film. They consist in ensuring that $\partial P/\partial\theta=\partial P/\partial Z=0$ and $P=0$ at the rupture limits of the film lubricant.
In the case of the present study, the bearing is operating under steady state conditions; the applied load F is constant and its direction is vertical. The total load W (supported by the contact) is calculated by integrating the pressure field along the surface contact of the journal bearing, then the attitude angle ϕ is obtained (Figure 1a).
The friction torques, ζ_1 on the journal and ζ_2 on the bearing, are respectively obtained by integrating the shearing stresses τ along the journal surface ($y=h$) and along the bearing surface ($y=0$). The axial fluid flow is obtained by integration of the speed component of the fluid in the axial direction z, and through the film section $ds=dxdy$.
All these characteristics are calculated numerically. The details of the calculations are reported in Frêne et al.[28]

2.1 Texture Shape

The texture shape used in this study is cylindrical. As shown on Figure 2, r_x, r_y and r_z are the dimensions of the texture, respectively in the x, y and z directions.

ISSN 2179-3956

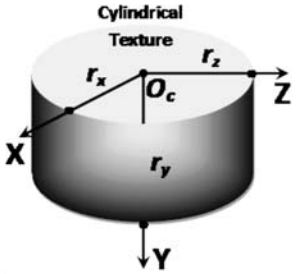

Figure 2. Cylindrical shape.

In the case of cylindrical dimple geometry, we have $r_x=r_z=r$ and the equation of geometry is defined by,

$$\left(x-x_c\right)^2+\left(z-z_c\right)^2=r^2 \tag{3}$$

The coordinates of the texture centre O_c are noted (x_c,y_c,z_c). This centre is located on the bearing surface, making $y_c=0$. The depth at point $M(\theta,Z)$ on the textured surface is defined by Δh (Figure 1b).

$$\Delta h = r_y \tag{4}$$

2.2 Resolution of the Reynolds Equation

The determination of the pressure in the lubricant film requires the numerical resolution of equation (1) using the Finite Difference Method. The most usual resolution method, used here, is that of Christopherson.[29] The resolution of linear systems obtained after discretisation is done by the iterative method of Gauss-Seidel. The use of an iterative method for the resolution is justified by the application of the Reynolds boundary conditions. The pressure is the only unknown, while the eccentricity is given (e.g. according to the difference between the given force F and that computated W, at the previous iteration step). This implies that equation (1) is the only one used to form the final equation system for obtaining P. The cavitation conditions must also be satisfied. For a steady-state regime, the computational procedure consists of giving initial values to the eccentricity $\varepsilon=e/C$. The pressure field is obtained verifying the pressure convergence condition $\left|\Delta P_i\right| / \left|P_i\right| \le \varepsilon_P$ at each nodal point i of the bearing surface. The supported load W and the bearing attitude angle ϕ are calculated. The calculated load and the external fixed load F are compared; the process stops when the load convergence condition $|F-W| / |F| \le \varepsilon_W$ is satisfied. If this error control is not satisfied, the eccentricity value is updated and the process of calculation is repeated.

3 RESULTS AND DISCUSSIONS

3.1. Computational Conditions

The eccentricity ratio used here, is kept to *0.60* (corresponds to external applied load of *12600 N*). One can remark that the pressure curves always stay under the

ISSN 2179-3956

pressure curve of the smooth case. A 3D textured model is illustrated in Figure 2. The shape of the dimples is chosen to be circular as this would be relatively easy to. A dimple is characterized by its radius (r) and depth (r_y) as shown in Figure 1(b). Bearing surfaces with cylindrical textures are analysed for the journal bearing shown in Figure 1a. The bearing surface is textured and stationary ($\omega_2=0$) while the journal surface is smooth and moving ($\omega_1 \neq 0$). Only one half of the journal bearing system is studied because of the symmetry of the bearing. Uniform meshes are used. The same geometrical parameters and operating conditions studied by Vincent, Maspeyrot and Frêne[30] are used here for the simulations.

- Magnitude of the external force F: 12600 N
- Angular speed of the shaft ω_1: 625.4 rad/s
- Shaft radius R: 0.0315 m
- Bearing length L: 0.063 m
- Radial clearance C: 0.00003 m
- Lubricant viscosity μ: 0.0035 Pa.s

In order to get mesh independent results, the grid used should be of fine quality. The grid resolution used for the smooth case is similar to that used for the dimpled cases. For the results presented below, the tests convergence precisions used for calculations of pressure P and load W are $\varepsilon_P=10^{-4}$ and $\varepsilon_W=10^{-5}$ respectively. The mesh size used is *891* nodes along circumferential direction and *142* nodes along axial direction.
In a recent work,[31] we have found that for specific texture distributions on the bearing surface and at higher asperity density, the texture has more influence on the contact characteristics.

Table 1. Characteristics of journal bearing without texture

Characteristics (Unit)	*This study*	*Vincent [31]*
Eccentricity	*0.601*	*0.600*
Amplitude of the external force F (N)	*12600*	*12600*
Attitude angle (°)	*50.4*	*50.2*
Maximum pressure (Mpa)	*7.7*	*7.0*
Minimum thickness 10^{-6} (m)	*11.96*	*12.00*
Axial flow 10^{-5} (m^3/s)	*1.74*	*1.73*
Friction torque (N.m)	*1.13*	-
Dissipated power (Watt)	*708.6*	-
Film rupture angle (°)	*203.5*	-

In relation to the journal bearing with smooth surfaces, the most important contact characteristics are computed. The results derived using the computational code of the authors,[31] was compared to those calculated by Vincent, Maspeyrot and Frêne.[30] Very good concordance between the results of the two studies is noted.

3.2 Results

Here, the cylindrical texture (*r=1 mm* and *ry=0.015 mm*) is used to investigate the texture distribution effect on the journal bearing characteristics. The eccentricity ratio is equal to *0.60* (Averagely loaded bearing). Circumferential coordinates θ_1, θ_2 and axial

ISSN 2179-3956

coordinates Z_1, Z_2 delimit the textures zone on the bearing surface. 25 cases are considered according to the geometric arrangement of textures on the bearing surface. Table 2 summarized the most important characteristics calculated for all these cases (the minimum film thickness h_{min}, the friction torque ζ, the fluid film flow Q, the attitude angle ϕ, the maximum pressure P_{max} and its angular position θ_m and finally the beginning of the cavitation zone θ_e).

Table 2. Textures distribution and calculated journal bearing characteristics

Case	θ_1 (°)	θ_2 (°)	Z_1	Z_2	h_{min} (μm)	ζ (N.m)	$Q\ 10^{-5}$ (m^3/s)	ϕ (°)	P_{max}/θ_m (Mpa / °)	θ_e (°)
0	*Untextured surface*				11.97	1.2173	1.743	50.5	7.71/148.0	203.5
1	0	360	0	0.500	8.71	1.3782	1.422	46.1	8.26/152.5	202.3
2	0	360	0	0.250	11.03	1.2555	1.515	49.1	8.36/150.1	201.8
3	0	360	0	0.125	11.70	1.2277	1.599	50.1	7.91/148.8	203.1
4	0	180	0	0.500	8.49	1.3940	1.432	47.1	8.40/152.5	195.4
5	0	180	0	0.250	10.99	1.2580	1.514	49.4	8.40/150.1	201.8
6	0	180	0	0.125	11.69	1.2281	1.598	50.1	7.92/148.8	203.1
7	0	90	0	0.500	11.75	1.2235	1.558	48.5	7.89/149.3	203.5
8	0	90	0	0.250	11.89	1.2194	1.627	49.8	7.77/ 148.4	203.5
9	0	90	0	0.125	11.94	1.2179	1.675	50.2	7.73/148.4	203.5
10	0	45	0	0.500	11.95	1.2175	1.700	50.2	7.72/148.4	203.5
11	0	45	0	0.250	11.96	1.2173	1.714	50.4	7.71/148.4	203.5
12	0	45	0	0.125	11.96	1.2173	1.725	50.4	7.71/148.4	203.5
13	180	360	0	0.500	12.16	1.2081	1.733	49.3	7.58/148.8	211.6
14	180	360	0	0.250	12.01	1.2152	1.742	50.2	7.67/ 148.4	203.9
15	180	360	0	0.125	11.97	1.2168	1.744	50.4	7.70/148.4	203.5
16	270	360	0	0.500	11.97	1.2173	1.743	50.5	7.70/148.4	203.5
17	90	191	0.153	0.403	9.68	1.3242	1.721	49.2	8.53/151.7	198.6
18	90	180	0.125	0.500	8.90	1.3708	1.737	49.3	7.74/151.2	195.8
19	180	270	0	0.500	12.16	1.2082	1.733	49.3	7.58/148.8	211.6
20	180	270	0.125	0.500	12.17	1.2081	1.731	49.3	7.58/148.8	212.0
21	180	270	0.125	0.375	12.07	1.2122	1.737	49.8	7.63/148.4	204.7
22	175	220	0.120	0.500	12.18	1.2067	1.729	49.0	7.56/148.8	215.2
23	180	225	0.200	0.500	12.11	1.2104	1.733	49.6	7.62/148.8	209.9
24	180	360	0.130	0.500	12.14	1.2091	1.732	49.4	7.60/148.8	211.6
25	185	230	0.120	0.500	12.19	1.2067	1.729	49.0	7.56/148.8	214.8

The Improvement of the journal bearing characteristics consists in increasing the minimum film thickness (have a better hydrodynamic load capacity), decreasing the friction torque (reduce the loss of energy by friction), improving the lubricant film presence region (have a better distribution of the pressure) and keeping the same value of the fluid film flow (maintain unchanged the value of the lubricant supply). The texture configuration 25 gives the best results compared with all the other cases, the minimum film thickness is increased by about 1.8%, the friction torque is reduce by about 1%.
Figure 3 shows the evolution of the minimal film thickness, the friction torque, the axial flow and the angle of rupture of the fluid film for the 25 cases of arrangement. For some cases, where the textures are totally located at the falling part of the pressure (case 13 to 16 and 19 to 25), the minimal film thickness increases, the friction torque decreases and the maximum pressure reduce fairly (max -1.9%). The pressure is sensibly diminished, however, the bearing performances are improved since the reduction of the cavitation zone (the limit of the rupture zone expands up to +5.6%) in the hydrodynamic

ISSN 2179-3956

contact. These configurations contain a texture located in the second angular part of the bearing (beyond 180°), at the declining part of the pressure curve.

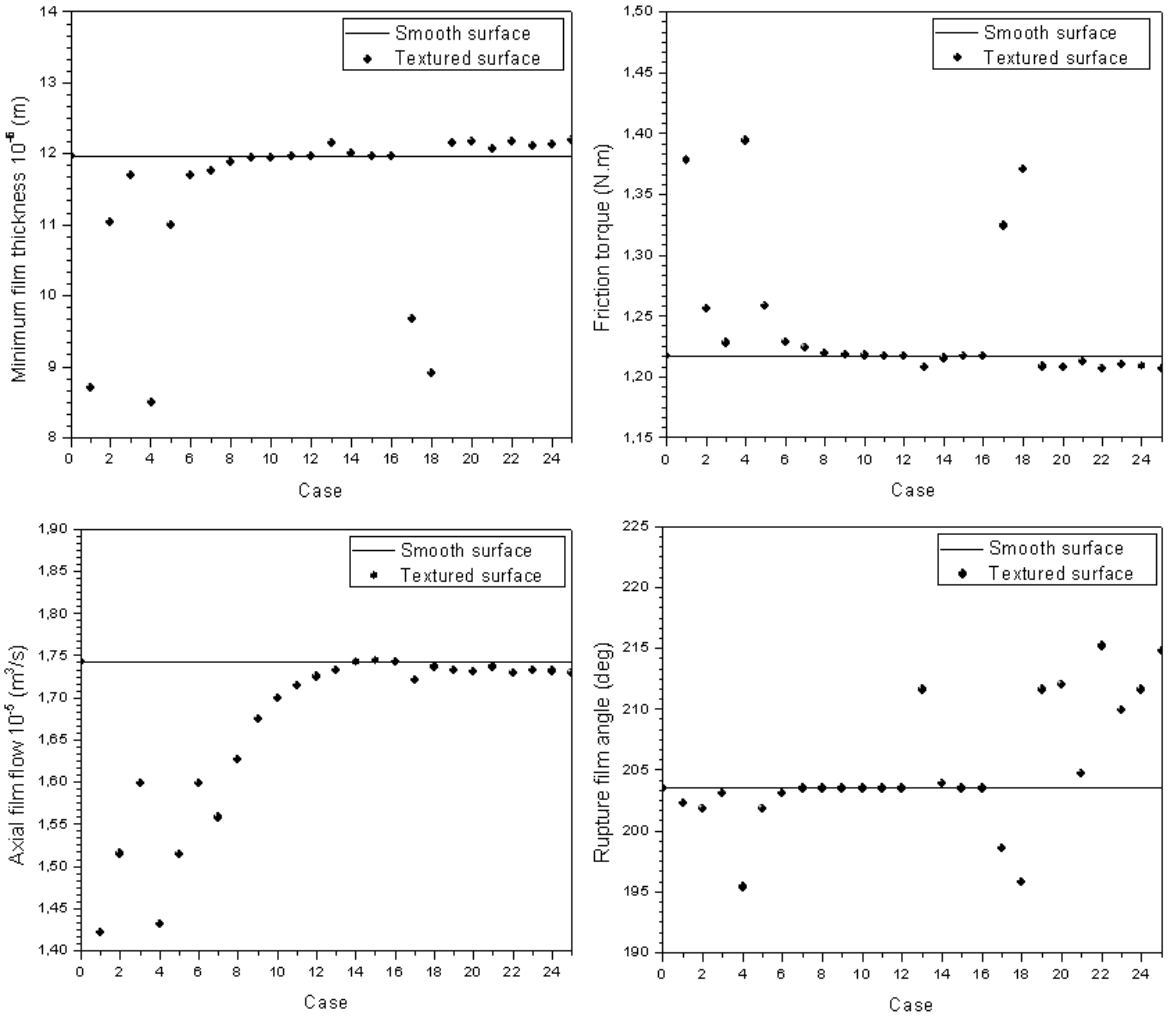

Figure 3. Variation of static characteristics for different distributions of textures on the bearing surface.

Texturing the outlet region of the contact located at the declining part of the pressure field, allows a better supply of the cavitation zone by film fluid. By consequence, a tiny decrease of the maximum pressure (until 1.9 %), of the fluid film flow (until 0.8 %) and of the friction torque in the contact (until 1 %) are noted. Expand the region of the fully film about 5.6% (corresponds to reduction of the cavitated zone) improve the pressure field distribution, the carrying-capacity are enhanced and the minimal film thickness is improved about 1.8%. The collective effect of the dimples in partial texturing gives an equivalent converging average film between the region of maximum pressure and the cavitation zone.

For cases 17 and 18 (eccentricity ratio equal to 0.60 and S = 0.8), textures are located in the first angular half of the bearing (between 0 and 180°). They correspond to textures area arrangements in the region of maximum pressure. For these configurations, the friction torque increases about 12.6%, the minimum film thickness decreases about

ISSN 2179-3956

25.6%, the maximum pressure rises about 10.6% and the zone of fully film fluid decreases about 3.8%. The configuration 17 gives a strong raise in maximum pressure (+10.6%), but a significant reduction in the film thickness (-19.1%) and a considerable augmentation in the friction torque (+8.8%) is observed. An increasing of the maximum hydrodynamic pressure (figure 6) does not lead automatically to an improvement of the journal bearing performances.

For the other cases (case 1 to 12), the value of the minimal film thickness decreases, the friction torque increases, the maximum pressure raises and the zone of complete film remain relatively constant. These configurations contain a texture located in the first angular part of the bearing (within 180°). The textures are situated at the inlet of the contact (near fluid supply and before 45°) for the cases 10 to 12, at the rising part of the pressure field for cases 7 to 9, at the rising part and maximum pressure region for the cases 4 to 6 and occupied the totality of the bearing surface for the cases 1 to 3.

Configurations 1 to 12 affect negatively the characteristics of the bearing. Texturing the contact inlet region (cases 10 to 12) has a modest and negative effect on the bearing performances; + 0.1% for the maximum pressure, -0.2% for the film thickness and no change is observed on the friction torque and the rupture angle. On the other hand, the flow film fluid is perturbed negatively and it decreases about 2.5%, which disturbs the cavitation zone supply by film fluid. For the cases from 1 to 9, the same thing is observed, just variations are more prominent. The most important variation is observed in the cases 1 and 4, which correspond to meshing the totality of the bearing and the first half part of this one (within 180°), respectively. Texturing the totality of the bearing surface (case 1), a half of this one (case 4) or a part (case 7) can lead to a consequent reduction in the performances of the journal bearing (figure 5).

The case 25 shows that it is possible to improve the performances. That confirms the importance of a good angular distribution of the textured zone on the bearing surface.

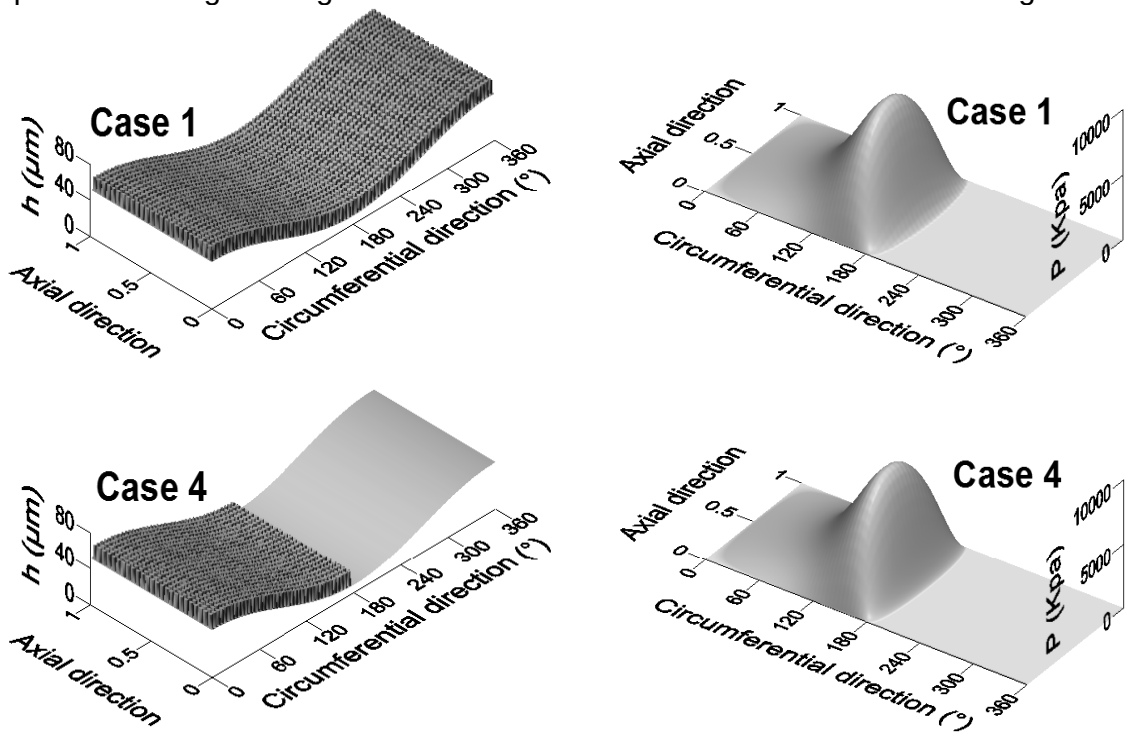

ISSN 2179-3956

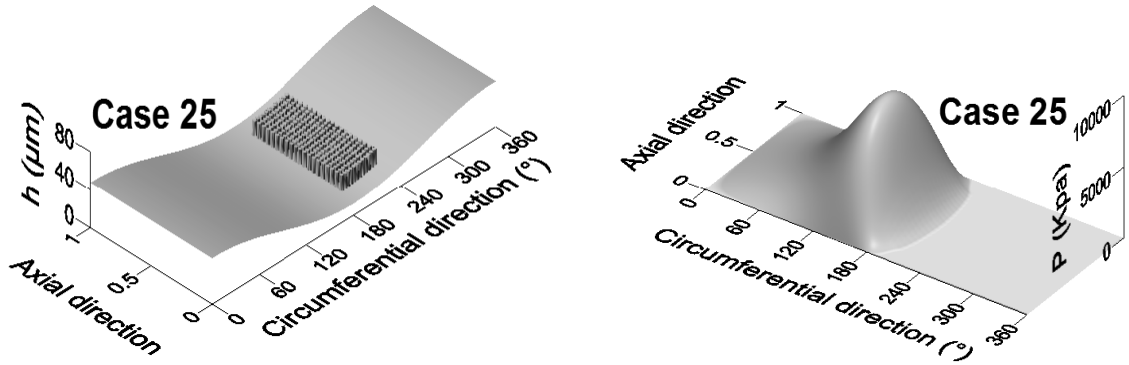

Figure 4. Variation of film thickness and pressure field for 3 cases of textures dispositions.

Figure 4 shows the variation of the minimal film thickness and the pressure for three distributions cases of textures on the bearing developed surface. The 3D cylindrical texture shape, its distribution on the contact surface and the angular position of the minimum film thickness (corresponding to the peak of pressure) can be obviously observed (near 150°).

4 CONCLUSIONS

A numerical model based on finite difference method was developed to study the textures distribution influence on the bearing surface of a hydrodynamic journal bearing subjected to a stationary load. The shaft (journal) is supposed to be smooth and rigid while the bearing surface is partially or totally textured with cylindrical texture shape. Different arrangements of the textured area have been considered. The presence of a cavity (texture) increases locally the lubricant film thickness and decreases the friction force.

Full texturing appears ineffective to generate hydrodynamic load capacity in the contact by the cavitation effects. Partial texturing can generate hydrodynamic lift in bearing, when the texture is located in the declining part of the contact pressure field.
In the complex case of a journal bearing, with both convergent (hydrodynamic pressure) and divergent (cavitation) zones, partial texturing has a minimal positive effect and full texturing has a negative effect. The textured area optimum design depends strongly on the geometrical parameters and the operating conditions of the journal bearing.

REFERENCES

1 Burton, R.A., Effects of two dimensional, sinusoidal roughness on the load support characteristics of lubricating film. Journal of Basic Engineering 84 (1963) 258-264.
2 Christensen, H., Stochastic models for hydrodynamic lubrication of rough surfaces. Proc Instn Mech Engrs 184(1) (1969-70) 1013-1025.
3 Patir, N., Cheng, H.S., Application of average flow model to lubrication between rough sliding surfaces. ASME Journal of Lubrication Technology 101 (1979) 220-230.
4 Lubrecht A.A., ten Napel W.E. and Bosma R., The influence of longitudinal and transverse roughness on the elastohydrodynamic lubrication of circular contacts. Journal of Tribology 110 (1988) 421-426.
5 Hargreaves, D.J., Surface waviness effects on the load carrying capacity of rectangular slider bearings. Wear 145 (1991) 137-151.

ISSN 2179-3956

6 Tonder, K., Dynamics of rough slider bearings: effects of one sided roughness/waviness. Tribology International 29(2) (1995) 117-122.
7 Letalleur, N., Plouraboue, F., Prat, M., Average flow model of rough surface lubrication: flow factors for sinusoidal surfaces. Journal of Tribology 124 (2002) 539-546.
8 Burstein, L., Two sided surface roughness and hydrodynamics pressure distribution in lubricating films. Lubrication Science 19(2) (2006) 101-112.
9 Priest, M., Taylor, C.M., Automobile engine tribology-approaching the surface. Wear 241 (2000) 193-203.
10 Wakuda, M., Yamauchi, Y., Kanzaki, S. and Yasuda, Y., Effect of Surface Texturing on Friction Reduction Between Ceramic and Steel Materials under Lubricated Sliding Contact. Wear 254 (2003) 356-363.
11 Etsion, I., State of the art in laser surface texturing. Journal of Tribology 127 (2005) 248-253.
12 Tonder, K., Inlet roughness tribodevices: Dynamic coefficient and leakage. Tribology International 34(12) (2001) 847-852.
13 Cupillard, S., Glavatskih, S., Cervantes, M. J., Computational fluid dynamics analysis of journal bearing with surface texturing. Proc. Instn Mech. Engrs, Part J: Journal of Engineering Tribology 222 (2008) 97-107.
14 Kovalchenko, O., Ajayi, A., Fenske Erdemir, G., and Etsion, I., The effect of laser surface texturing on transitions in lubrication regimes during unidirectional sliding contact. Tribology International 38 (2005) 219-225.
15 Siripuram, R.B., Stephens, L.S., Effect of Deterministic Asperity Geometry on Hydrodynamic Lubrication. Journal of Tribology 126 (2004) 527-534.
16 Buscaglia, G.C., Ciuperca, I., Jai, M., The effect of periodic textures on the static characteristics of thrust bearings. Journal of Tribology 127 (2005) 899-902.
17 Fowel, M., Olver, A.V., Gosman, A.D., Spikes, H.A., Pegg, I., Entrainment and inlet suction: two mechanisms of hydrodynamic lubrication in textured bearings. J. of Tribology 129 (2007) 336-347.
18 Brahamani, R., Shirvani, A., Shirvani, H., Optimization of partially textured parallel thrust bearings with square-shaped micro-dimples. Tribology Trans. 50 (2007) 401-406.
19 Murthy A.N., Etsion I., Talke, F.E., Analysis of surface textured air bearing sliders with rarefaction effects. Tribology Letters 28 (2007) 251-261.
20 Tala-ighil, N., Maspeyrot, P., Fillon, M., Bounif, A., Effects of surface texture on journal bearing characteristics under steady state operating conditions. Proc. Instn Mech. Engrs, Part J: J. Engineering Tribology 221(16) (2007) 623-634.
21 De Kraker, A., Ostryen, R. A. J., Van Beek, A., Rixen, D. J., A multiscale method modelling surface texture effects. J. Tribol., 129 (2007) 221-230.
22 Cupillard, S., Glavatskih, S., Cervantes, M.J., Pressure build up mechanism in a textured inlet of a hydrodynamic contact. Journal of Tribology 130(2) (2008).
23 Cupillard, S., Glavatskih, S., Cervantes, M.J., Inertial effects in textured hydrodynamic contacts. Proc. Instn Mech. Engrs, Part J: Journal of Engineering Tribology 224 (2010).
24 Buscaglia, G. C., Ciuperca, I., and Jai, M. On the optimization of surface textures for lubricated contacts. J. Math. Anal. Appl., 335 (2007) 1309–1327.
25 Brizmer,V.,Klingerman,Y., and Etsion, I. A laser surface textured parallel thrust bearing. Tribol. Trans., 46 (2003) 397–403.
26 Dobrica, M. B. and Fillon, M. About the validity of Reynolds equation and inertia effects in textured sliders of infinite width. Proc. IMechE, Part J: J. Engineering Tribology, 223 (2009) 69–78.
27 Dobrica, M. B., Fillon, M., Pascovici, M. D., Cicone, T., Optimizing surface texture for hydrodynamic lubricated contacts using a mass-conserving numerical approach. Proc. Instn Mech. Engrs, Part J: Journal of Engineering Tribology 224 (2010).

ISSN 2179-3956

28 Frêne, J., Nicolas, D., Degueurce, B., Berthe, D. and Godet, M., Hydrodynamic lubrication bearings and thrust bearings. In Tribology series 33 (Ed. D. Dowson) (Elsevier, London, UK) 1997.
29 Christopherson, D.G., A new mathematical method for the solution of film lubrication problems, Institute of Mechanical Engineering. J. Proc. 146 (1941) 126-135.
30 Vincent, B., Maspeyrot, P., Frêne, J., Starvation and Cavitation Effects in Finite Grooved Journal Bearing. Proc. Of the 21st Leeds-Lyon Symposium on Tribology, Lubricants and Lubrication, Tribology serie 30, session 'Machine Elements'. September (1994) 455-464.
31 Tala-ighil, N., Maspeyrot, P., Fillon, M., Bounif, A., Hydrodynamic effects of texture geometries on journal bearing surfaces. The Annals of University "Dunarea de Jos" of Galati, Fascicle VIII, ISSN 1221-4590, Tribology, XIV (2008) 47-52.